EUROPEAN FUSION DEVELOPMENT AGREEMENT

EFDA–JET–CP(03)01-34

P. U. Lamalle, M.-L. Mayoral, I. Monakhov
and JET EFDA Contributors

Three-Dimensional Modelling of the JET A2 ICRH Antenna

Three-Dimensional Modelling of the JET A2 ICRH Antenna

P. U. Lamalle[1], M.-L. Mayoral[2], I. Monakhov[2]
and JET EFDA Contributors

[1]Laboratory for Plasma Physics, Association EURATOM - Belgian State, Trilateral Euregio Cluster, Royal Military Academy, 30 av. de la Renaissance, B-1000 Brussels, Belgium.
[2]EURATOM – UKAEA Fusion Association, Culham Science Centre, Abingdon OX14 3DB, U.K.
**See Annex of J. Pamela et al., "Overview of Recent JET Results and Future Perspectives", Fusion Energy 2000 (Proc. 18th Int. Conf. Sorrento, 2000), IAEA, Vienna (2001).*

Preprint of Paper to be submitted for publication in Proceedings of the
EPS Conference on Controlled Fusion and Plasma Physics,
(St. Petersburg, Russia, 7-11 July 2003)

ABSTRACT.

Antenna codes developed by the ICRH community include fairly realistic descriptions of wave propagation in magnetized plasmas, but rather crude representations of the launcher. This may seriously limit the accuracy of the resulting input impedance matrix, which is an essential ingredient of coupling predictions. Successful quantitative predictive modelling of the coupling characteristics of RF structures as complex as the JET A2 arrays remains to be demonstrated (the experimental coupling resistance Rc of these antennae being less than their design estimate of the early nineties). The recent appearance of highly powerful and versatile commercial electromagnetic codes has brought hope to make decisive progress, although these products do not yet include a magnetized plasma. We have taken this approach, and report on recent three-dimensional electromagnetic modelling of the JET A2 ICRF antennae using the MICROWAVE STUDIO® (MWS) software [3]. This work was triggered by renewed interest in accurate predictions of ICRH antenna array coupling during the design activity of the JET ITER-Like antenna. Our goals are to validate the numerical simulations against available A2 experimental data, to understand the array RF characteristics in detail, and to improve confidence in predictions for future designs.

1. MODEL AND FIRST SIMULATION RESULTS

The main features of the antenna are reproduced from its drawing office blueprints [2]: curved geometry, thick folded straps and their short-circuits, antenna box, septa, all the tilted Faraday shield elements, feeders, Figure 1. The machine wall is simulated by a metal back plane. The study is ongoing, and we present results for halfthe array (straps #3 and 4) in two configurations: shielded radiating in vacuum (Figures 3 to 6), and unshielded radiating in a high-permittivity dielectric mimicking single-pass wave launch in a plasma (Figures 2 and 6). Each MWS simulation (based on a time-domain analysis and Fourier transform of the results) covers the frequency response up to ~120MHz, well exceeding the operational domain (23 to 57MHz). Figure 2 illustrates the current densitypeaking in areas of high curvature (dipole phasing case): strap edges, folds near the short-circuits, and the significant image currents in the antenna box sides. The resulting radiation spectrum has larger high-k// components than assumed in early simulations. The case of monopole phasing (not shown) also exhibits strong image currents in the central septum, as expected. A significant fraction of the current flows on the back side of the straps, i.e. 4.8cm behind the front side. Both features contribute to explain a lower radiation in the plasma with respect to simpler (thin strap, uniform current, box-free) models.

Figure 3 shows two-dimensional levels of electric field in vertical planes through each strap. The gradual voltage increase along the Faraday shields from short circuits toward feeds is clearly visible. Local field concentrations near cylindrical shield elements and in narrow gaps are resolved numerically.

The total current flowing along the straps is computed from the 3D full-wave solutions, and shown as a function of curvilinear abscissa along all main conductor segments on Figure 4. Extensive analysis of these results will be reported elsewhere.

2. COMPARISON WITH 1995 MEASUREMENTS ON ANTENNA PROTOTYPE

The simulated two-by-two input reactance matrix in vacuum is in fair agreement with laboratory measurements on half an antenna, Figure 5. Least-squares fits to the results of Figures 4 and 5 (for a given voltage phasing and balance at the input ports) yield simple equivalent circuits for each strap (over the operating frequency range), made of two transmission line sections connected in parallel onto a feed line. More elaborate equivalent circuits, made of mutually coupled elements and valid for arbitrary port excitations, are also under development. Upper and lower sections of the inner strap have similar characteristic impedances estimated ~32W, for a cross-over conductor characteristic impedance ~38W (these figures are preliminary, and subject to revision as the analysis is ongoing). In contrast, there seems to be a significant characteristic impedance imbalance between upper and lower sections of the outer strap, which manifests itself strongly above 70MHz. This important feature, together with differences in electrical length, are responsible for the experimental difference in frequency response between inner and outer straps.

A preliminary comparison of antenna strap coupling resistances between the available simulations and laboratory measurements is illustrated on the left diagram of Figure 6: the frequency dependences qualitatively agree when sufficient loading is present in the simulations, but a proper comparison remains to be carried out by including foam loading and RF losses in the model.

3. FORTHCOMING MODELLING

The most important outstanding issue in this work is the validation of computed resistive loading against available experimental data, such as the JET ICRH coupling database (right part of Figure 6, relative to whole 4-strap arrays), recent network analyzer measurements in situ, and 1995 scattering matrix studies on plasma [7]. The realism of the simulations can be improved in various respects, first of all by addressing the complete 4-strap array and introducing RF losses. Several routes for improving simulations of plasma loading are under investigation: the most satisfactory one pursues ‘first principle’ simulations. It requires implementation of a magnetized plasma in MWS and availability of plasma edge density profile data. An alternative is to calibrate an ad-hoc ‘equivalent dielectric’ in MWS to fit the experimental results. Although of lesser scientific interest, this approach can provide invaluable information on the expected performance of the future JET ITER-Like launcher. A third possibility is to use the detailed current patterns obtained by MWS as sources in the available plasma coupling and heating codes. The present simulations also allow in-depth analysis of complex launcher features, such as the Faraday shield current patterns, to be reported in the future.

CONCLUSIONS

For the first time, the high level of geometrical detail included in A2 ICRH antenna simulations has enabled computation of near field and reactive properties, with unprecedented accuracy and from first principles. Fair agreement is found between numerical vacuum reactances and earlier measurements on half an A2 antenna with foam loading. A realistic description of reactive properties

is essential in coupling predictions. The frequency dependence of the A2 coupling resistance is well understood in terms of reactive effects and simple equivalent circuits. Work is actively proceeding to bring the description of resistive loading on a similar level.

ACKNOWLEDGEMENTS

Stimulating discussions with Ing. F. Durodié and Dr. J.-M. Noterdaeme are gratefully acknowledged. This work has been performed under the European Fusion Development Agreement.

REFERENCES

[1]. Pécoul, S., et al, Comp. Phys. Comm. **146** (2002) 166-187.

[2]. Kaye, A., et al, Fusion Engineering and Design **24** (1994) 1.

[3]. CST MICROWAVE STUDIO User Manual, Version 4.0, CST GmbH, Darmstadt, Germany, 2002; http://www.cst-world.com

[4]. Durodié, F., et al, (2003) Proc. 15th Topical Conference on Radio Frequency Power in Plasmas, Moran, U.S.A.

[5]. Lamalle, P. U., et al, (2003) Proc. 15th Topical Conference on Radio Frequency Power in Plasmas, Moran, U.S.A.

[6]. Fechner, B., Optimisation des antennes radio-fréquences A2 pour le chauffage cyclotronique ionique sur le tokamak JET, Ph.D. Thesis, Université Aix-Marseille I (1996).

[7]. Lamalle, P.U., et al, Europhysics Conference Abstracts **19C** (1995) II 329-332 (Proc. 22nd EPS Conference on Controlled Fusion and Plasma Physics, Bournemouth, U.K.)

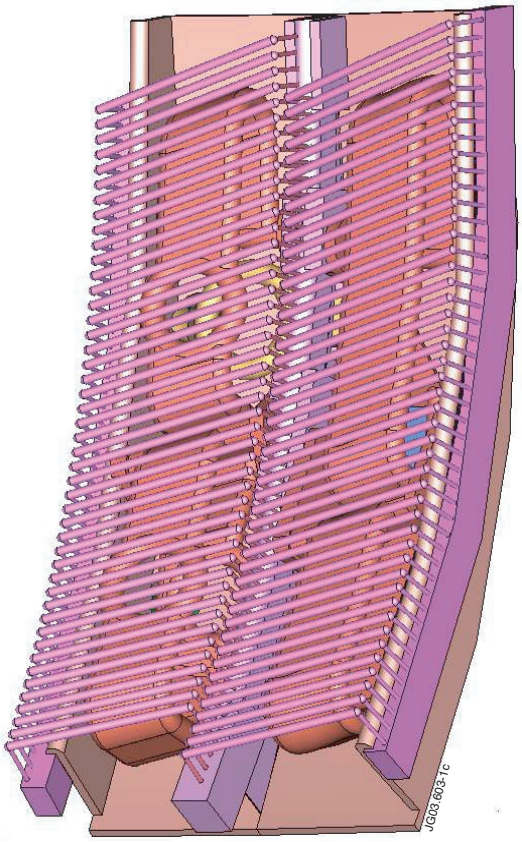

Figure 1: MWS model of half a JET A2 antenna. Left: strap #4 ('outer'); right: strap #3 ('inner'), fed by an in-vessel 'crossover' conductor. Feeders are at a common toroidal location behind strap 4.

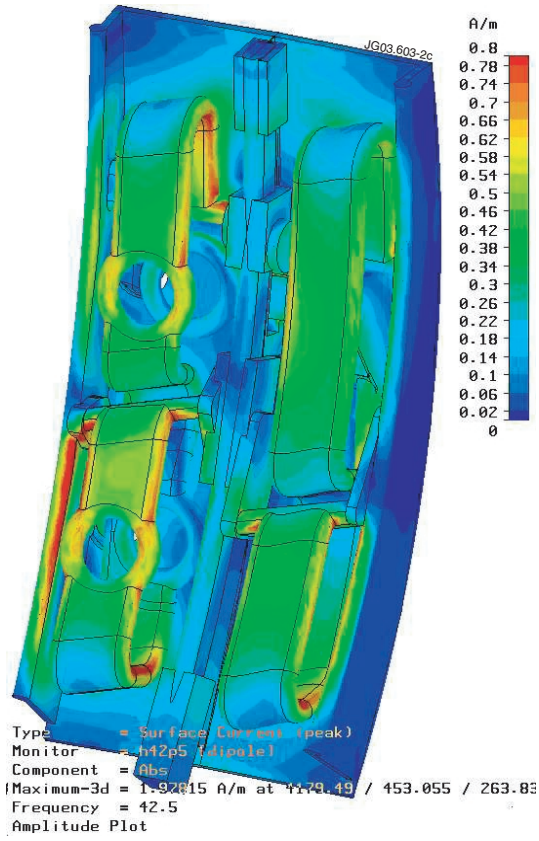

Figure 2: Amplitude of surface current density in dipole phasing at 42.5MHz (unshielded case with dielectric loading). Arbitrary units, with dark blue corresponding to 0 and red maximum

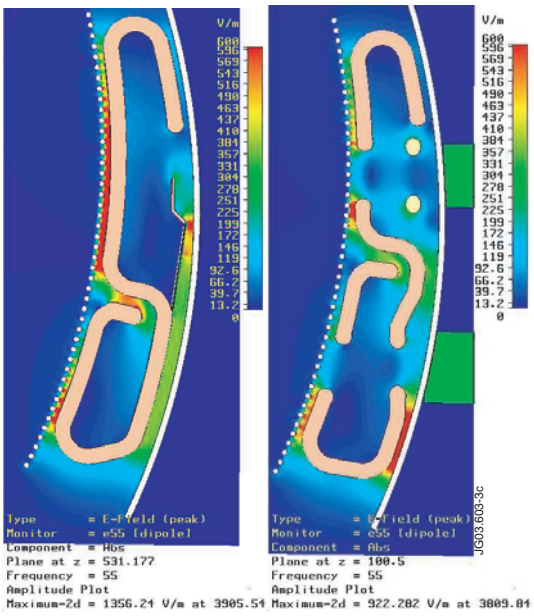

Figure 3: RF electric field amplitude in vertical cut planes through straps #3 (left) and 4 (right). Shielded antenna in vacuum, 55MHz, dipole phasing. Arbitrary units, with dark blue corresponding to 0 and red to maximum.

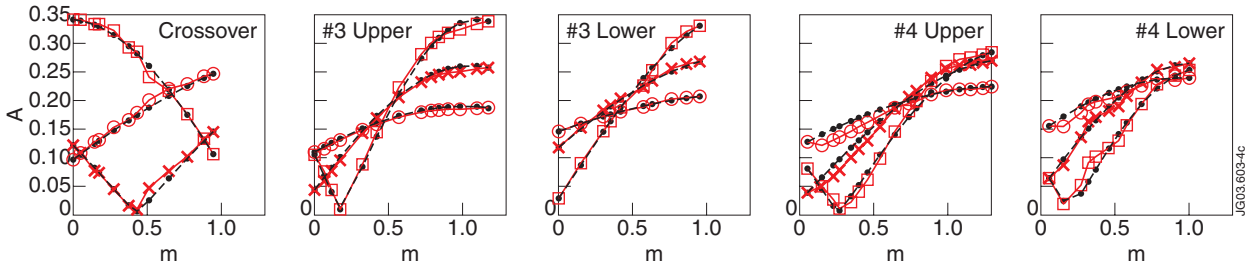

Figure 4: Computed current amplitude along each strap section at 30, 42.5 and 55MHz (resp. symbols o, ×,) and best fit by equivalent transmission lines in that frequency range (black dots). Dipole phasing, Faraday shield on. N.B. the abscissa limits do not exactly coincide with the ends of the sections. □

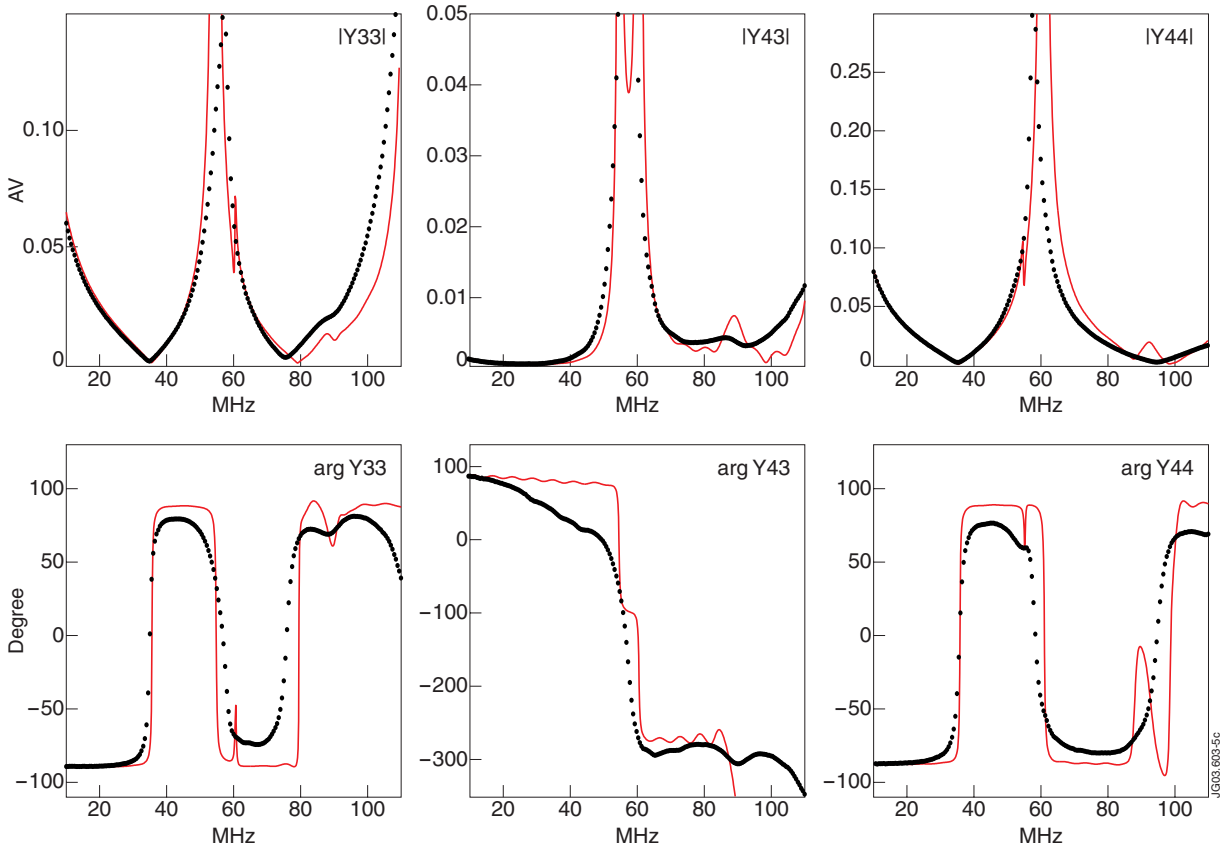

Figure 5: Input admittance matrix element vs. frequency. Upper row: amplitude; lower row: phase in degree. Black dotted lines: from 1995 network analyzer measurements by Fechner [6] on A2 prototype loaded with absorbing tiles; red plain lines: MWS vacuum simulation (shield on).

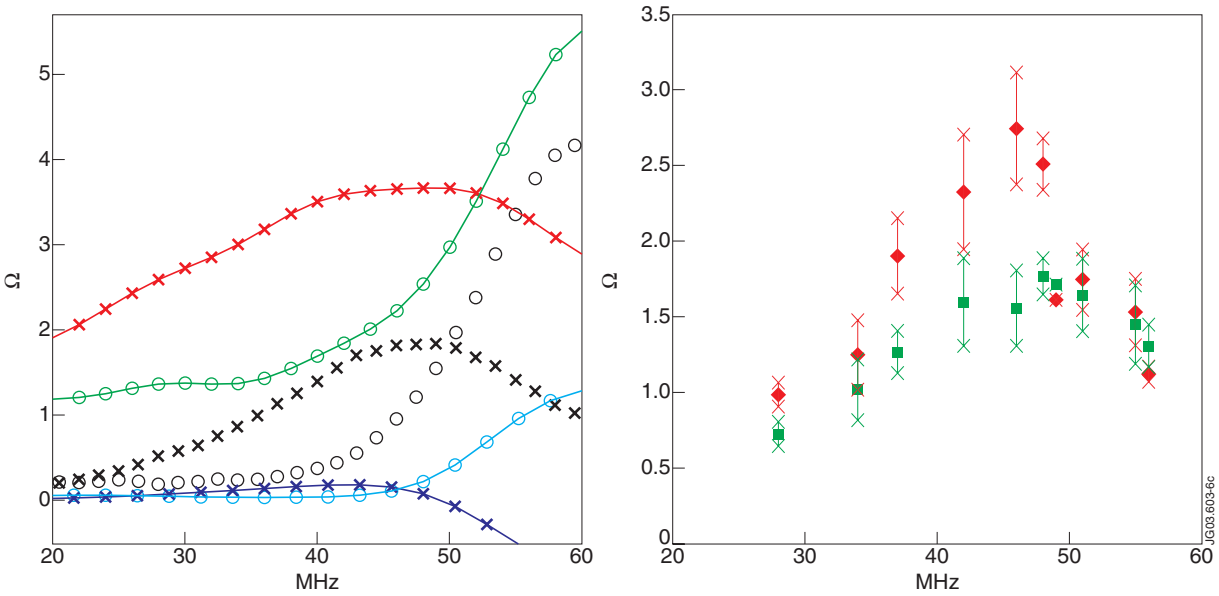

Figure 6: Left: coupling resistance Rc (ohm) versus frequency in dipole phasing for inner (o) and outer (×) straps. Black symbols: from prototype measurements with foam loading of [6]; colored lines: from two MWS simulations. Lower curves (blue and cyan): vacuum with shield, no RF losses. Upper curves (red and green): dielectric loading, no shield. Right: coupling resistance Rc versus frequency for inner ( ) and outer (o) straps in dipole phasing. From JET A2 coupling database on plasma, average over the 4-strap arrays A and B, ELMy H Mode, MkIIa divertor, $3<q_{95}<4.5$, 3<ROG(cm)<4, RF line losses subtracted. The error bars indicate one standard deviation on either side of the average.